

Negative thermal expansion of ReO_3 : Neutron diffraction experiments and dynamical lattice calculations

Tapan Chatterji,¹ Paul F. Henry,² R. Mittal,^{3,4} and S. L. Chaplot⁴

¹Jülich Centre for Neutron Science, Forschungszentrum Jülich Outstation at Institut Laue-Langevin, BP 156, 38042 Grenoble Cedex 9, France

²Institut Laue-Langevin, BP 156, 38042 Grenoble Cedex 9, France

³Forschungszentrum Jülich, Jülich Centre for Neutron Science, c/o TU München, Lichtenbergstrasse 1, D-85747 Garching, Germany

⁴Solid State Physics Division, Bhabha Atomic Research Centre, Trombay, Mumbai 400085, India

(Received 30 May 2008; revised manuscript received 4 September 2008; published 8 October 2008)

We have investigated the temperature variation of the unit-cell volume of ReO_3 by neutron diffraction. The lattice parameter and the unit-cell volume decrease continuously as the temperature is increased from $T = 2$ K to about $T = 200$ K. After exhibiting minima at about 200 K they increase with increasing temperature linearly up to about 305 K, the maximum temperature investigated during the present experiment. We attribute the negative thermal expansion of ReO_3 to be the results of rigid antiphase rotations of the neighboring ReO_6 octahedra. We have done model lattice dynamical calculation of phonon dispersions, thermal expansion, and atomic displacement parameters in ReO_3 . The results of these calculations are in agreement with the experimental results.

DOI: [10.1103/PhysRevB.78.134105](https://doi.org/10.1103/PhysRevB.78.134105)

PACS number(s): 61.05.fm, 65.40.De

Transition-metal oxides have been the subject of renewed interest ever since high-temperature superconductivity was discovered in copper oxide materials. The transition-metal oxides with narrow d bands form strongly correlated Mott-Hubbard system for which conventional band theory is no longer valid.¹ The number of transition-metal oxides, where band theory alone can provide adequate account of their properties, is quite limited, and is confined to compounds of the $4d$ and $5d$ series. ReO_3 is an example of such a simple metallic oxide. Among d -electron conductors ReO_3 has a simple perovskite-like cubic structure and its conductivity is comparable to that of Ag. Although the electron-phonon coupling constant is not very small² (the coupling constant $\lambda = 0.34$) ReO_3 surprisingly does not show superconductivity down to 20 mK. ReO_3 seems to belong to the normal class of conventional band Fermi liquids with electron-phonon interactions dominating the resistivity.² ReO_3 crystallizes in the cubic space group ($Pm\bar{3}m$) with the undistorted perovskite-like DO_6 -type structure with lattice constant $a = 3.74$ Å. The structure consists of corner-linked ReO_6 octahedra with Re at the centers and linear Re-O-Re links. Among the numerous perovskite-like compounds ReO_3 belongs to a small family of undistorted cubic structures, which is stable at ambient pressure and at all temperatures up to its melting point. Also the ReO_3 structure has a completely vacant A cation site of the ABO_3 perovskite structure. This empty structure is therefore expected to allow rigid rotation of the ReO_6 octahedra.³⁻⁵

High pressure x-ray and neutron-diffraction measurements⁶⁻⁸ established that ReO_3 undergoes a pressure-induced second-order phase transition at $P_c = 5.2$ kbar at room temperature to a tetragonal ($P4/m\bar{b}m$) intermediate phase with a very narrow stability range in pressure and then a further transition to a cubic ($\text{Im}\bar{3}$) phase. The driving force of the phase transition was shown to be the softening of the M_3 phonon mode involving rigid rotation of the ReO_6 octahedra, and the octahedral rotation angle was identified as an order

parameter of the phase transition.^{7,8} Further pressure-induced phase transitions at higher pressures have been reported.⁹⁻¹¹ We determined the pressure-temperature phase diagram¹² of ReO_3 in temperature range 2–300 K in the medium pressure range up to about 7 kbar from our neutron-diffraction investigation on a ReO_3 single crystal. The pressure-induced structural phase transition in ReO_3 has been recently investigated by x-ray-absorption fine structure.¹³ This investigation suggests that even at ambient pressure Re-O-Re bond angle is not 180° but is about 170° . ReO_3 only appears cubic in a time-averaged and space-averaged structures obtained by the conventional diffraction analysis of the Bragg intensities. The local nanoscale structure of ReO_3 seems to be distorted. Similar conclusions were drawn by Rechav *et al.*¹⁴ from the x-ray absorption fine structure spectra of antiferro-distortive perovskites, $\text{Na}_{0.82}\text{K}_{0.18}\text{TaO}_3$ and NaTaO_3 . The simultaneous Rietveld and pair distribution function (PDF) analysis¹⁵ of the high-temperature phase transition in $\alpha\text{-AlF}_3$ also suggests that the high-temperature cubic perovskite phase may also be distorted at the nanoscale level.

The cubic perovskite structure in ReO_3 is essentially unstable due to the softening of the M_3 phonon mode involving rigid rotation of the ReO_6 octahedra. Although the average crystal structure appears cubic, the real nanoscale local structure may be more complex. The rigid unit modes (RUM) involved in the structural instability should lead to negative thermal expansion (NTE).¹⁶ We therefore investigated the temperature dependence of the lattice parameter of ReO_3 by neutron diffraction. We found indeed the negative thermal expansion in ReO_3 at low temperatures. The lattice parameter and the unit-cell volume decrease continuously as the temperature is increased from $T = 2$ K to about $T = 200$ K. After exhibiting a minimum at about 200 K they increase linearly up to about 305 K, the maximum temperature investigated.

The NTE, i.e., the decrease in volume or length of a material with increasing temperature is an unusual property ex-

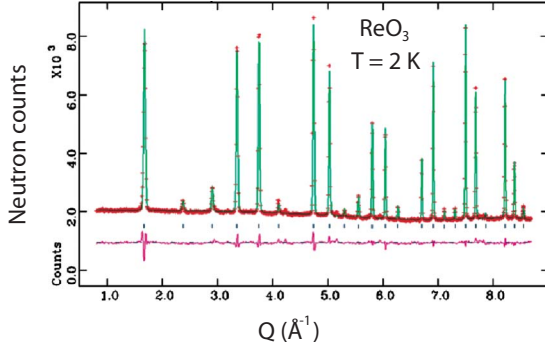


FIG. 1. (Color online) Diffraction intensity of ReO_3 as a function of $Q=4\pi \sin \theta/\lambda$ measured at $T=2$ K on the diffractometer D20 of the Institut Laue-Langevin along with the results of Rietveld refinement.

hibited by relatively few materials.^{16–20} The phenomenon NTE can arise from a range of different mechanism, viz., magnetostriction, valence transition, anharmonicity of low-energy phonon modes, etc. Here we are concerned with the anharmonicity of low-energy phonon modes which is believed to be the origin of the NTE in oxide-based framework materials.^{16,21–25} The NTE materials have generated significant scientific and commercial interest because they can be used to compensate the more usual positive thermal expansion (PTE) of usual materials. In order to understand the negative thermal expansion behavior in ReO_3 , we have also carried out lattice dynamical calculation. Our calculations show that the negative thermal expansion of ReO_3 is due to the unusually large anharmonicity of the soft M3 mode, which consists of rigid antiphase rotations of the neighboring ReO_6 octahedra.

We have organized the paper in the following way. In Sec. II we give the experimental neutron-diffraction methods and then describe the results. In Sec. III we give lattice dynamical calculations and discuss the experimental results using the results of these calculations. Finally in Sec. IV we give a summary of the results and conclusions.

Neutron-diffraction measurements on ReO_3 powders were done on diffractometer D20²⁶ at the Institut Laue-Langevin in Grenoble. The dry polycrystalline sample was put inside a vanadium can and was sealed and was placed inside an Orange-type He cryostat of the diffractometer. The diffraction intensities from ReO_3 were measured in the temperature range 1.7–305 K. The neutron wavelength was determined to be $\lambda=1.359 \pm 0.001$ Å from the wavelength calibration measurement with NIST Si640b as a standard.

Figure 1 shows a typical diffraction diagram of ReO_3 measured at $T=2$ K along with the results of the Rietveld profile fit. The diffraction intensity is plotted here as a function of the momentum transfer $Q=4\pi \sin \theta/\lambda$ rather than 2θ . The Re and O atoms in ReO_3 structure ($Pm3m$) occupy special positions [Re: $(1a)000$; O: $(3d)\frac{1}{2}00$] and have no positional fit parameters in the cubic $Pm3m$ phase. So only the lattice parameter, the thermal displacement parameters of Re and O atoms, and the scale factor were refined. The agreement factor R was about 2%. Figure 2(a) shows the temperature variation of the cubic lattice parameter a . The lattice

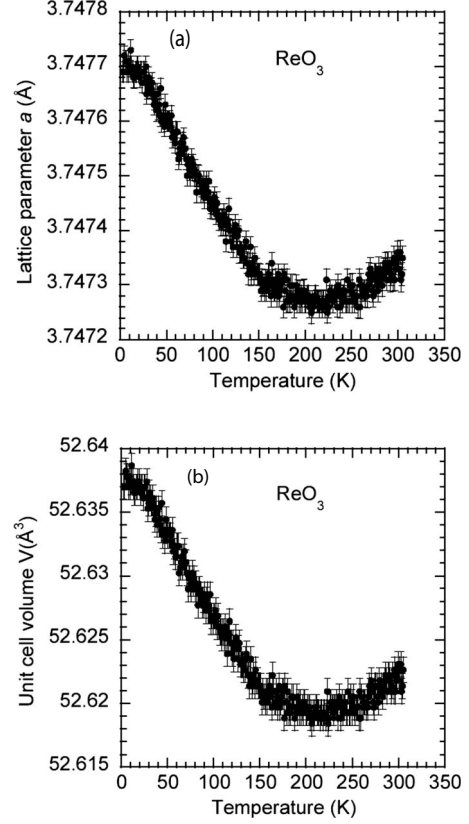


FIG. 2. Temperature variation of the (a) lattice parameter and (b) the unit-cell volume of ReO_3 . The continuous lines are guides to the eye.

parameter decreases continuously as the temperature is increased from $T=2$ K to about $T=200$ K and exhibits a minimum at about this temperature. At higher temperature the lattice parameter a increases with increasing temperature in a normal way. The temperature variation of the unit-cell volume of cubic ReO_3 shown in Fig. 2(b) behaves similarly. The total volume contraction from 2 to 200 K is about 0.036% and is rather small, but is much larger than the experimental error. This is the demonstration of the negative thermal expansion in ReO_3 by diffraction measurements. Matsuna *et al.*²⁷ reported earlier negative thermal expansion below about 300 K by measuring thermal expansion only at a few isolated temperatures by the laser beam interference method in the temperature range 100–500 K. The present data are much more extensive than that reported by Matsuna *et al.*²⁷

Figure 3 shows the temperature variation of the thermal displacement parameters of Re and O atoms. The point-group symmetries of the special positions occupied by Re ($1a$) and O ($3d$) atoms allow only isotropic thermal displacement parameters U for Re, while O atoms can have anisotropic thermal displacement parameters with two components $U_{11}=U_{\parallel}$ and $U_{22}=U_{33}=U_{\perp}$, which represent vibrations parallel and perpendicular to the Re-O bond, respectively. The U of Re and $U_{11}=U_{\parallel}$ of O are small, are of the same order of magnitude, and have similar temperature variation whereas the $U_{22}=U_{33}=U_{\perp}$ of the O atom is much larger and increases strongly with temperature. Thus the O

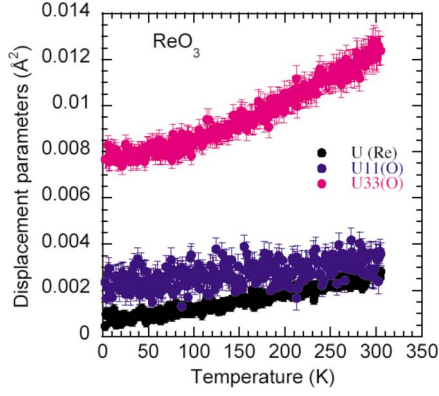


FIG. 3. (Color online) Temperature variation of the thermal displacement parameters of the Re and O atoms of ReO_3 .

atoms in ReO_3 have highly anisotropic thermal vibrations. The large thermal vibration amplitude U_{\perp} perpendicular to the Re-O bond direction is consistent with the soft M_3 phonon mode. The thermal displacement obtained by us compares well with the previously reported values⁸ measured at $T=300$ K up to a much larger value of Q also on a powder ReO_3 sample but at a spallation neutron source. The temperature dependence of the thermal displacement parameters also agrees very well with that measured by single crystal x-ray diffraction.²⁸

The lattice dynamical calculations are carried out using the following interatomic potential:

$$V(r) = \left(\frac{e^2}{4\pi\epsilon_0} \right) \left\{ \frac{Z(k)Z(k')}{r} \right\} + a \exp \left\{ \frac{-br}{R(k) + R(k')} \right\}, \quad (1)$$

where r is the distance between the atoms of types k and k' . The parameters of interatomic potential are the effective charge $Z(k)$ and radius $R(k)$ of the atom type k , $a = 1822$ eV, and $b = 12.364$. The parameters used in our calculations are $R(\text{Re}) = 0.72$ Å, $R(\text{O}) = 1.87$ Å, $Z(\text{Re}) = 2.40$, and $Z(\text{O}) = -0.80$. We have also included a covalent potential between the nearest Re and O atoms,

$$V(r) = -D \exp[-n(r - r_0)^2/2r]. \quad (2)$$

The parameters of the stretching potential are $D = 6.4$ eV, $n = 4.4$ Å⁻¹, and $r_0 = 1.875$ Å. The polarizability of the O atoms is introduced in the framework of the shell model^{29,30} with the shell charge $Y(\text{O}) = -1.2$ and shell-core force constant $K(\text{O}) = 135$ eV Å⁻². The parameters satisfy the static and dynamic equilibrium conditions of the lattice. The parameters were fitted to the available structural and dynamical data at ambient pressure and then used in calculations as a function of pressure. The calculated value of lattice parameter 3.7476 Å of the cubic cell at ambient pressure is in good agreement with the experimental value of 3.7477 Å. The crystal structure at any pressure (at zero temperature) is obtained by minimization of the enthalpy. The current version of the program DISPR (Ref. 31) has been used for the lattice dynamical calculations.

In quasiharmonic approximation the volume thermal expansion coefficient is given by

$$\alpha_V = \frac{1}{BV} \sum_i \Gamma_i C_{Vi}(T), \quad (3)$$

where V is the unit-cell volume, B is the bulk modulus, and $\Gamma_i = d \ln \omega_i / d \ln V$ and C_{Vi} are the mode Grüneisen parameter and specific-heat contribution, respectively, of the phonons in state $i(=\mathbf{q}_i)$ of frequency ω_i . It is worth noting that anomalous thermal expansion occurs because Γ_i , which reflects the dependence of the frequency ω_i on volume, is very different for different modes. Otherwise, the coefficient of thermal expansion would closely follow the variation of the specific heat, as happens in many materials. We calculated the thermal expansion by integrating over the contribution of phonons of 165 wave vectors in the irreducible Brillouin zone. The contribution to thermal expansion^{32,33} arising from the variation of bulk modulus with temperature has also been included. The detailed procedure for the lattice dynamical calculations and various thermodynamic properties is given in our previous publications.^{34,35}

ReO_3 has a cubic structure with space group $Pm\bar{3}m$ and one formula unit per primitive cell. The group theoretical analysis of phonon dispersion relation for ReO_3 at Γ point, and along the Δ and Σ directions, has been carried out using standard techniques.^{30,36} The 12 phonon modes along $[110]$ and $[100]$ and at Γ point can be classified as

$$\Gamma: 3T_{1u} + T_{2u}, \quad (4)$$

$$\Delta: 3\Delta_1 + 1\Delta_3 + 4\Delta_5, \quad (5)$$

$$\Sigma: 4\Sigma_1 + \Sigma_2 + 4\Sigma_3 + 3\Sigma_4, \quad (6)$$

where T_{1u} and T_{2u} are triply degenerate and Δ_5 's are doubly degenerate. T_{1u} modes are infrared active and T_{2u} modes are silent. Axe *et al.*⁷ determined the phonon dispersions of the low-energy transverse and longitudinal acoustic phonon modes of ReO_3 by inelastic neutron scattering. Both the transverse $T_1(\xi 00)$ and $T_2(\xi \xi 0)$ modes have anomalous low frequencies extending to the zone boundaries. But the most remarkable feature is the pronounced reduction in frequency of the T_2 mode near the M -point zone boundary $(1/2, 1/2, 0)$. Figure 4 shows our model calculations of the phonon dispersion of ReO_3 along with the experimental data obtained from inelastic neutron scattering.⁷ The agreement appears to be satisfactory. In particular, the acoustic modes slopes have been very well reproduced and the soft mode at M point has also been calculated qualitatively. Here we have used a simple model that has the essential physics. As we shall see, the present model is able to identify the important phonon modes associated with the anomalous thermal expansion behavior and almost quantitatively account for it. The agreement with experiments can be improved with a more complex model with more adjustable parameters.

The calculated value of the bulk modulus for ReO_3 is 210 GPa, which is in very good agreement with the reported experimental value³⁷ of 211 GPa. The Grüneisen parameter $\Gamma(E)$ averaged for all phonons of energy E has been calculated using pressure dependence of phonon spectra and is shown in Fig. 5 (top). The calculations show that $\Gamma(E)$ has small positive values for phonons of energy up to 15 meV.

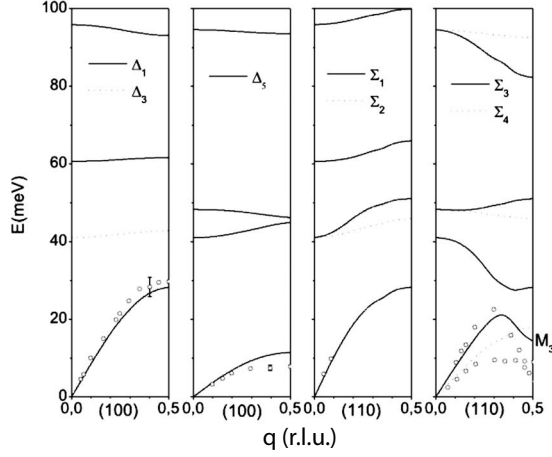


FIG. 4. Comparison between the calculated (lines) and experimental data (Ref. 7) (symbols) of phonon dispersion relation for ReO_3 .

For energies around 20 ± 5 meV phonons have average negative $\Gamma(E)$ values in the range of -3 and -1 . It can be seen that there is significant energy dependence of $\Gamma(E)$. We have used this energy dependence of $\Gamma(E)$ for the calculation of volume thermal expansion coefficient using Eq. (3). The small values of $\Gamma(E)$ for the low-energy modes result in a small value of thermal expansion coefficient below 25 K and this is shown in Fig. 5 (bottom). This is followed by the negative expansion at higher temperature similar to that determined by the neutron-diffraction experiments. The calculations yield positive $\Gamma(E)$ values for modes above 50 meV,

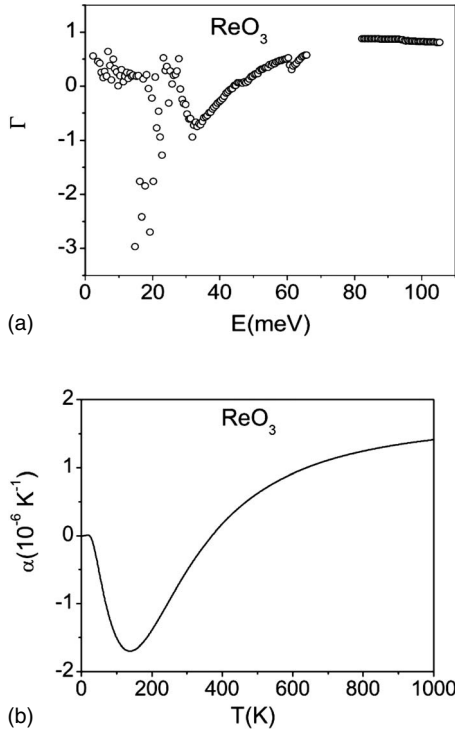


FIG. 5. Calculated (a) Grüneisen parameter $\Gamma(E)$ averaged over phonons of energy E and (b) volume thermal expansion coefficient α_V in ReO_3 .

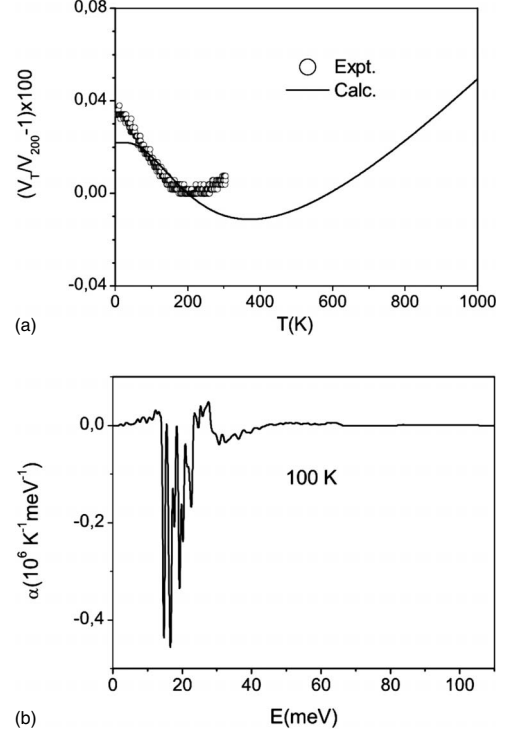


FIG. 6. (a) Comparison between the calculated and experimental thermal expansion behavior of ReO_3 . (b) Contribution of phonons of energy E to the volume thermal expansion as a function of E at 100 K in ReO_3 .

which results in a positive volume thermal expansion coefficient above 350 K. This result is in agreement with the experiments where negative to positive expansion crossover occurs at 200 K.

Figure 6 (top) shows a comparison between the calculated and experimental thermal expansion behavior in ReO_3 . The calculation gives a minimum of volume at about 350 K whereas experimentally the minimum in unit-cell volume is at about 200 K. Otherwise the agreement is good. In Fig. 6 (bottom) we show the average contribution of various phonons of certain energy E to the thermal expansion as function of E at 100 K. The maximum negative contribution to α_V arises from the modes of energy around 14 meV. The energy of about 14 meV corresponds to the M_3 mode at the zone boundary along $[110]$. This mode is plotted (Fig. 7) using the calculated eigenvector, which shows librational

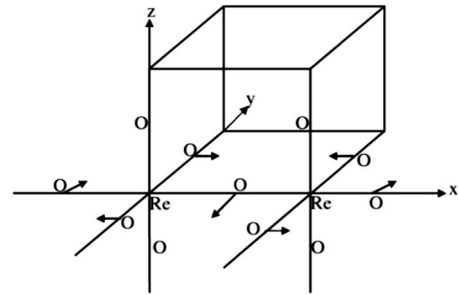


FIG. 7. Polarization vector of the M_3 mode involving rotation of ReO_6 octahedra in the $a-b$ plane.

motion of ReO_6 octahedron arising from the transverse vibrations of the O atoms in the a - b plane. Axe *et al.*⁷ have also measured the pressure dependence of this phonon and found it to decrease substantially with increasing pressure, which yields the Grüneisen parameter Γ_{M3} of the $M3$ phonon to be about -225 for pressures between 1 bar and 1 kbar. The exact value depends strongly on the pressure, and in particular, on the difference between the pressure of the measurement and the phase-transition pressure. In comparison, our calculation yields the value of -11 . For ReO_3 the large negative value of the Grüneisen parameter for the $M3$ phonon mode essentially leads to the negative thermal expansion at low temperatures where the low-energy $M3$ phonon mode dominates. Similar negative thermal expansion has been observed²⁵ in Si and Ge for which the Grüneisen parameter Γ_i is negative for certain acoustic modes. The acoustic modes dominate the thermal expansion coefficient at low temperatures because of their relatively large contribution to the specific heat.

The calculated partial phonon densities of states have been used to calculate the mean squared amplitudes of Re and O atoms in ReO_3 as a function of temperatures. The comparison between our calculations and experimental data is shown in Fig. 8. The amplitudes of the oxygen atoms are highly anisotropic; the value perpendicular to the Re-O bond ($U33$) is much larger than that along the bond ($U11$). However, $U33$ as observed at very low temperatures is large, which may indicate static disorder of the oxygen atoms perpendicular to the Re-O bond. Such a static disorder has been indicated by previous x-ray absorption fine structure (XAFS) measurements as discussed in Sec. I. The calculations yield only the thermal amplitudes, which appear to be in good agreement with experiments if the static component is subtracted. Also the absolute values of the thermal displacement parameters obtained from the refinement of powder neutron-diffraction data measured up to only $Q \approx 8.5 \text{ \AA}^{-1}$ are not very reliable especially in the presence of the static components that cannot be separated from the dynamic components. To get accurate values of thermal displacement parameters one should measure diffraction intensities up to a much higher value of Q by using shorter wavelength. Nevertheless

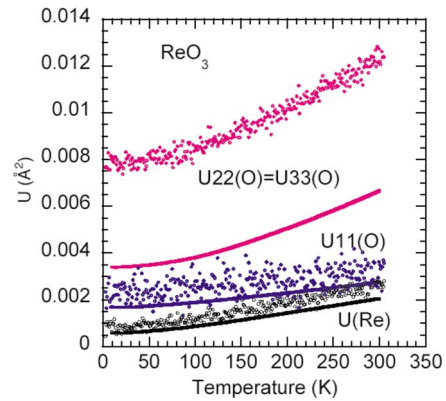


FIG. 8. (Color online) Comparison between the calculated (lines) and experimental (symbols) thermal displacement parameters of ReO_3 . The black symbol and line give observed and calculated $U(\text{Re})$, whereas blue and red symbols and lines correspond to the observed and calculated values of $U11(\text{O})$ and $U22(\text{O}) = U33(\text{O})$.

the large anisotropy of the $U11$ and $U33$ for the O atoms and also the amplitude of the Re atom have been well reproduced by the calculations.

We have done powder neutron-diffraction investigation of the temperature variation of the average structure of ReO_3 . We measured neutron-diffraction intensities with very fine temperature steps in the temperature range from 2 to 305 K and have determined the temperature variation of the lattice parameter and the unit-cell volume of ReO_3 and have discovered negative thermal expansion in the low-temperature range 2–200 K. Above about 200 K the thermal expansion becomes positive and remains so up to 305 K, the highest temperature of the present investigation. We ascribe the negative thermal expansion of ReO_3 at low temperatures to the negative Grüneisen parameter of the zone boundary M_3 phonon mode representing the antiphase rotation of the neighboring ReO_6 octahedra. Our model lattice dynamical calculations are in good agreement with the experimental results.

¹P. Fulde, *Electron Correlation in Molecules and Solids* (Springer-Verlag, Berlin, 1991).

²P. B. Allen and W. W. Schulz, *Phys. Rev. B* **47**, 14434 (1993).

³F. S. Razavi, Z. Altounian, and W. R. Datars, *Solid State Commun.* **28**, 217 (1978).

⁴J. E. Schirber and B. Morosin, *Phys. Rev. Lett.* **42**, 1485 (1979).

⁵B. Batlogg, R. G. Maines, M. Greenblatt, and S. DiGregorio, *Phys. Rev. B* **29**, 3762 (1984).

⁶J. E. Schirber, B. Morosin, R. W. Alkire, A. C. Larson, and P. J. Vergamini, *Phys. Rev. B* **29**, 4150 (1984).

⁷J. D. Axe, Y. Fujii, B. Batlogg, M. Greenblatt, and S. Di Gregorio, *Phys. Rev. B* **31**, 663 (1985).

⁸J. E. Jørgensen, J. D. Jørgensen, B. Batlogg, J. P. Remeika, and J. D. Axe, *Phys. Rev. B* **33**, 4793 (1986).

⁹J.-E. Jørgensen, S. Olsen, and L. Gerward, *J. Appl. Crystallogr.* **33**, 279 (2000).

¹⁰E. Suzuki, Y. Kobayashi, S. Endo, and T. K. Ikegawa, *J. Phys.: Condens. Matter* **14**, 10589 (2002).

¹¹J.-E. Jørgensen, W. G. Marshall, R. I. Smith, J. Staun Olsen, and L. Gerward, *J. Appl. Crystallogr.* **37**, 857 (2004).

¹²T. Chatterji and G. J. McIntyre, *Solid State Commun.* **139**, 12 (2006).

¹³B. Houser and R. Ingalls, *Phys. Rev. B* **61**, 6515 (2000).

¹⁴B. Rechav, Y. Yacoby, E. A. Stern, J. J. Rehr, and M. Newville, *Phys. Rev. Lett.* **72**, 1352 (1994).

¹⁵P. J. Chupas, S. Chaudhuri, J. C. Hanson, X. Qiu, P. L. Lee, S. D. Shastri, S. J. L. Billinge, and C. P. Grey, *J. Am. Chem. Soc.* **126**, 4756 (2004).

- ¹⁶For a review, see J. S. O. Evans, *J. Chem. Soc. Dalton Trans.* **19**, 3317 (1999).
- ¹⁷E. Grüneisen, *Handb. Sens. Physiol.* **10**, 1 (1926).
- ¹⁸A. W. Sleight, *Annu. Rev. Mater. Sci.* **28**, 29 (1998).
- ¹⁹A. W. Sleight, *Nature (London)* **389**, 923 (1997).
- ²⁰G. D. Barrera, J. A. O. Bruno, T. H. K. Barron, and N. L. Allan, *J. Phys.: Condens. Matter* **17**, R217 (2005).
- ²¹Y. M. Hao, Y. Gao, B. W. Wang, J. P. Qu, Y. X. Li, F. Hu, and J. C. Deng, *Appl. Phys. Lett.* **78**, 3277 (2001).
- ²²J. R. Salvador, F. Gu, T. Hogan, and M. G. Kanatzidis, *Nature (London)* **425**, 702 (2003).
- ²³T. A. Mary, J. S. O. Evans, T. Vogt, and A. W. Sleight, *Science* **272**, 90 (1996).
- ²⁴A. K. A. Pryde, K. D. Hammonds, M. T. Dove, V. Heine, J. D. Gale, and M. C. Warren, *J. Phys.: Condens. Matter* **8**, 10973 (1996).
- ²⁵J. Li, A. Yokachi, T. G. Amos, and A. W. Sleight, *Chem. Mater.* **14**, 2602 (2002).
- ²⁶T. C. Hansen, P. F. Henry, H. E. Fischer, J. Torregrossa, and P. Convert, *Meas. Sci. Technol.* **19**, 034001 (2008).
- ²⁷N. Matsuno, M. Yoshimi, S. Ohtake, T. Akahane, and N. Tsuda, *J. Phys. Soc. Jpn.* **45**, 1542 (1978).
- ²⁸M. Morinaga, K. Sato, J. Harada, H. Adachi, S. Ohba, and Y. Saito, *J. Phys. C* **16**, L177 (1983).
- ²⁹P. Bruesch, *Phonons: Theory and Experiments I* (Springer-Verlag, Berlin, 1982).
- ³⁰G. Venkatraman, L. Feldkamp, and V. C. Sahni, *Dynamics of Perfect Crystals* (MIT, Cambridge, 1975).
- ³¹S. L. Chaplot (unpublished).
- ³²V. K. Jindal and J. Kalus, *Phys. Status Solidi B* **133**, 89 (1986).
- ³³R. Bhandari and V. K. Jindal, *J. Phys.: Condens. Matter* **3**, 899 (1991).
- ³⁴S. L. Chaplot, N. Choudhury, S. Ghose, M. N. Rao, R. Mittal, and P. Goel, *Eur. J. Mineral.* **14**, 291 (2002).
- ³⁵R. Mittal, S. L. Chaplot, and N. Choudhury, *Prog. Mater. Sci.* **51**, 211 (2006).
- ³⁶O. V. Kovalev, *Irreducible Representations of Space Groups* (Gordon and Breach, New York, 1964); C. J. Bradley and A. P. Cracknell, *The Mathematical Theory of Symmetry in Solids* (Oxford University press, Oxford, 1972).
- ³⁷N. Tsuda, Y. Sumino, I. Ohno, and T. Akahane, *J. Phys. Soc. Jpn.* **41**, 1153 (1976).